BIOCHEMISTRY
including biophysical chemistry & molecular biology

Article

pubs.acs.org/biochemistry

Functional Characterization of *Staphylococcus epidermidis* IcaB, a De-*N*-acetylase Important for Biofilm Formation

Varvara Pokrovskaya,[†] Joanna Poloczek,[†] Dustin J. Little,[‡,§] Heather Griffiths,[†] P. Lynne Howell,[‡,§] and Mark Nitz*[,†]

[†]Department of Chemistry, University of Toronto, Toronto, Ontario M5S 3H6, Canada

[‡]Program in Molecular Structure & Function, Research Institute, The Hospital for Sick Children, Toronto, Ontario M5G 1X8, Canada

[§]Department of Biochemistry, University of Toronto, Toronto, Ontario M5S 1A8, Canada

Supporting Information

ABSTRACT: A polymer of partially de-*N*-acetylated β-1,6-linked *N*-acetylglucosamine (dPNAG), also known as the polysaccharide intercellular adhesin (PIA), is an important component of many bacterial biofilm matrices. In *Staphyloccocus epidermidis*, the poly-*N*-acetylglucosamine polymer is partially de-*N*-acetylated by the extracellular protein IcaB. To understand the mechanism of action of IcaB, the enzyme was overexpressed and purified. IcaB demonstrates metal-dependent de-*N*-acetylase activity on β-1,6-linked *N*-acetylglucosamine oligomers with a broad preference for divalent metals. Steady-state kinetic analysis reveals the low catalytic efficiency (pentasaccharide k_{cat}/K_M 0.03 M^{-1} s^{-1}) of the enzyme toward the oligomeric substrates. While IcaB displays similar rates of de-*N*-acetylation with tri- through hexasaccharide PNAG oligomers, position specific de-*N*-acetylation was only observed with penta- and hexasaccharides. The enzyme preferentially de-*N*-acetylates the second residue from the reducing terminus in the pentasaccharide and second and third residues from the reducing terminus in the hexasaccharide. The data described here represent an important step toward a detailed understanding of dPNAG biosynthesis in *S. epidermidis*, an important nosocomial pathogen, as well as in other Gram-positive bacteria. The low catalytic activity of IcaB is consistent with reports of other enzymes which act on biofilm-related polysaccharides, and this emerging trend may indicate a common feature among this group of polysaccharide processing enzymes.

Biofilms are surface-attached cellular communities of bacteria that surround themselves with a secreted matrix.[1,2] The formation of a biofilm significantly increases bacterial tolerance toward antibacterial agents and the host's defenses.[3] Estimates suggest that over 65% of human microbial infections are biofilm related.[4] Exopolysaccharides are often key components of the biofilm matrix.[1] Exopolysaccharides act as a structural support, as an adhesin, as a barrier against the hosts immune system and play a key role in bacterial self-organization.[5,6]

A polymer of partially de-*N*-acetylated β-1,6-linked *N*-acetylglucosamine (dPNAG) has emerged as a major biofilm matrix exopolysaccharide in *Staphylococcus epidermidis*[7] and *aureus*[8] as well as in many Gram-negative bacteria[1,9−15] (Figure 1). The Gram-positive bacteria *S. aureus* and *S. epidermidis* are the most frequent causes of nosocomial infections on indwelling medical devices.[16] In these bacteria dPNAG is likely the most important biofilm matrix component.[1] The proteins responsible for dPNAG production in *S. epidermidis* are encoded by the *icaADBC* genes.[17−21] IcaA and IcaD are membrane proteins and, together, are required for maximal GlcNAc polymerization from UDP-GlcNAc.[20] IcaC is predicted to be an integral membrane protein responsible for the export of the growing polymer.[21] IcaB is predicted to contain a single de-*N*-acetylase domain with characteristics of the family 4 carbohydrate esterases (CE4), as defined by the CAZy database.[22] CE4 family members are characterized by metal-dependent deacetylase activity and a conserved His-His-Asp

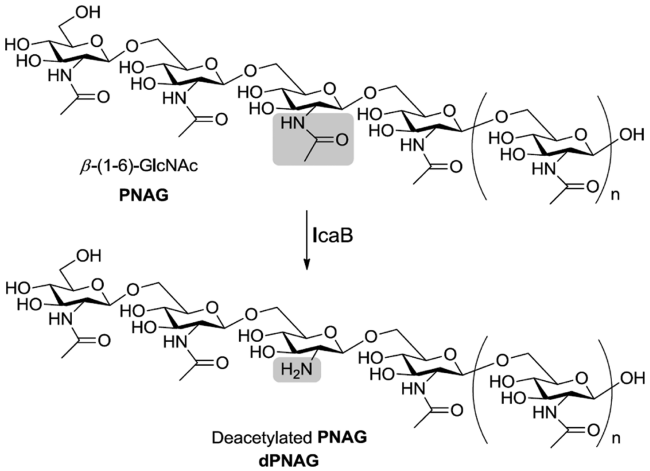

Figure 1. Reaction catalyzed by IcaB and the structure of PNAG.

Received: June 27, 2013
Published: July 18, 2013

   dx.doi.org/10.1021/bi400836g | *Biochemistry* 2013, 52, 5463−5471

metal ligating triad. Immunofluorescence microscopy has shown that IcaB is associated with the bacterial surface, and the protein has also been detected in cell culture medium.[17,21] Transposon mutagenesis of IcaB supports its activity as a β-1,6-linked *N*-acetylglucosamine (PNAG) de-*N*-acetylase which acts on PNAG postpolymerization.[21] Deletion mutants of IcaB in *S. epidermidis* and *S. aureus* have dramatically reduced biofilm formation *in vitro* as well as reduced pathogenicity in animal models of biofilm infections, suggesting this enzyme is a potential therapeutic target for antibiofilm therapies.[8,21]

Recent structural and biochemical analysis of the *Escherichia coli* homologue of IcaB, PgaB, revealed a two domain protein with an N-terminal de-*N*-acetylase domain and a putative C-terminal carbohydrate binding domain.[23,24] PgaB was most active with Co^{2+}, Fe^{2+}, or Ni^{2+} metal cofactors. IcaB is homologous (24% identity, 55% similarity) to the N-terminal de-*N*-acetylase domain of PgaB. In the present study, we demonstrate the activity of IcaB on PNAG substrates with recombinant protein. While PgaB and IcaB both have de-*N*-acetylase activity toward the oligomeric PNAG substrates they differ in their metal cofactor preference and substrate recognition. These differences reflect upon the activity requirements of the two proteins in the extracellular matrix (IcaB) and periplasm (PgaB), respectively.

MATERIALS AND METHODS

Materials. Competent BL21 (DE3) and XL2-blue *E. coli* cells were purchased from Strategene. Recombinant IcaB (residues 30−289) was codon optimized and cloned into a pET-16b expression vector between the NdeI and *Bam*HI restriction sites by BioBasic Inc. to yield plasmid UT032. Superdex 75 gel filtration resin was from Amersham Pharmacia Biotech, Ni(II)-nitrilotriacetic acid (NTA) agarose resin was purchased from QIAGEN, and Chelex 100 resin was purchased from BioRad. Most reagents used were purchased from Sigma-Aldrich. Metal salts were a minimum of 99.9% pure. All buffers for metal assays were treated with Chelex 100 to minimize trace metal contamination. Milli-Q (Millipore) distilled deionized water was used to prepare all buffers and growth media.

Overexpression and Purification of Recombinant His-Tagged $IcaB_{His10}$. Competent BL21 (DE3) *E. coli* cells were transformed using heat shock with the UT032 plasmid. Overnight cultures were used to inoculate 1L of LB media supplemented with 100 mg/L ampicillin, and the cultures were grown at 37 °C to an OD_{600} of 0.5. The cells were cooled to 10 °C, allowed to grow until OD_{600} 0.7−0.9, and induced with a final concentration of 0.75 mM isopropyl β-D-thiogalactoside (IPTG). Preliminary experiments demonstrated that the addition of 1 mM Ni^{2+} or Zn^{2+} to the medium led to significantly lower protein yields, so they were not added to subsequent preparations. After 24 h at 10 °C, the cells were harvested by centrifugation (3430*g* for 40 min at 4 °C). The cell pellet from 1L of media was suspended in 20 mL of buffer A (20 mM sodium phosphate, pH 7, 1 M NaCl, 5% (v/v) glycerol) and subjected to sonication on ice (10 s pulses with a 10 s rest between pulses, eight times). The crude extract was centrifuged to remove cell debris (16260*g* for 40 min at 4 °C). The supernatant was gently mixed with 0.5 mL of Ni(II)-NTA resin (QIAGEN) for 1 h before being loaded into a column (1 cm diameter). All purification steps were performed at 4 °C. Unbound proteins were washed from the resin with 10 mL of buffer A containing 20 mM imidazole. $IcaB_{His10}$ was eluted with buffer A containing 150 mM imidazole. The purified protein was dialyzed overnight against buffer A, washed with buffer B (50 mM sodium phosphate, pH 8, 500 mM NaCl) by centrifugation in an Amicon Ultra-15 10 000 Da MWCO centrifugal filter (Millipore), and concentrated to 3 mg/mL. The purity of the protein as analyzed by 15% sodium dodecyl sulfate−polyacrylamide gel electrophoresis (SDS-PAGE) was >95%. The protein was stored in buffer B at 4 °C. Protein mass was confirmed by electrospray ionization mass spectrometry (ESI-MS). The protein concentrations were determined using a molar extinction coefficient of 39 400 M^{-1} cm^{-1} calculated from a BCA assay on purified protein.

Preparation of IcaB. The purified $IcaB_{His10}$ was digested with Factor Xa protease (New England Biolabs, Ipswich, MA) according to the suggested protocol. Briefly, 1 mg of $IcaB_{His10}$ was incubated with 9 μg of Factor Xa at room temperature for 4 h in FXa reaction buffer (75 mM HEPES, pH 6.5, 75 mM NaCl, 100 mM Na_2SO_4, 2 mM $CaCl_2$). After protease digestion, Factor Xa protease was removed from the reaction mixture by affinity chromatography using Xarrest Resin. Xarrest resin slurry (100 μL, pre-equilibrated with FXa reaction buffer) was added to the cleavage reaction. The resin was resuspended by gentle mixing and incubated for 10 min at room temperature with slow rotation. The mixture was centrifuged for 5 min at 1000*g* and the supernatant collected. In order to remove cleaved His-tag peptide, the sample was washed 4 times on 10 000 MWCO centrifugal filter with buffer B. The effectiveness of the digestion was analyzed by SDS-PAGE.

Size Exclusion Chromatography. 50 μL of 1 mg/mL $IcaB_{His10}$ (IcaB) was run at 0.25 mL/min on Superdex 75 column (Amersham Pharmacia Biotech) equilibrated with buffer B. Gel filtration standards (BioRad) were used to calculate protein molecular weight (thyroglobulin (bovine), 670 kDa; γ-globulin (bovine), 158 kDa; ovalbumin (chicken), 44 kDa; myoglobin (horse), 17 kDa; vitamin B12, 1.35 kDa).

PNAG Substrate Preparation. Oligomers of β-1,6-*N*-acetylglucosamine were synthesized and purified as described previously.[25] The identity of the oligosaccharides was confirmed by MALDI-MS and ^{1}H NMR spectroscopy. Oligosaccharides were stored as lyophilized powders at room temperature and dissolved with deionized water or buffer as required. The concentrations of the PNAG oligomers were determined by ^{1}H NMR spectroscopy with an internal standard of dimethylformamide (DMF).

Assay Methods for Enzyme Activity. The enzymatic activity of IcaB was measured with a fluorescamine discontinuous assay with PNAG substrate (a mixture of GlcNAc tetramer and pentamer)[26] or a continuous fluorogenic assay with 3-carboxyumberlliferyl acetate (ACC) as a substrate.[27] Standard reactions for the fluorescamine assay consisted of 30 μM enzyme in buffer B, 30 μM $CoCl_2$, and 50 mM PNAG substrate in a total volume of 25 μL. Purified $IcaB_{His10}$ or IcaB and $CoCl_2$ were preincubated at room temperature for 1 h. PNAG oligomer was then added to a final concentration of 50 mM, and immediately after mixing, 10 μL of sample was removed and frozen (t = 0). The remaining assay mixture was incubated at 37 °C for 24 h prior to removal of a second 10 μL of sample. The pH of all samples was adjusted to pH 9 by adding 20 μL of 0.5 M borate buffer, and the samples were reacted with 10 μL of fluorescamine solution (20 mg/mL in DMF). After incubation for 10 min at room temperature, 40 μL of deionized water was added, and the samples were transferred to a Corning 3686 half-area 96-well black plate. Fluorescence was quantified by using a TECAN Safire2 plate

reader with excitation and emission wavelengths of 360 and 460 nm, respectively. The production of free amine was quantified using a glucosamine standard.

For the steady-state initial velocity kinetics purified GlcNAc trimer and pentamer were used as substrates, and the substrate concentrations were varied from 10 to 200 mM. The fluorescence intensity data were analyzed by using nonlinear regression analysis with Grafit,[28] with the default equations for first-order reaction rates and Michaelis−Menten steady-state kinetics. All measurements were performed in triplicate.

For the continuous fluorogenic assay 30 μM purified $IcaB_{His10}$ in buffer B and 30 μM $CoCl_2$ were incubated at room temperature for 30 min. The mixture was then incubated with the corresponding concentration of 3-carboxyumberlliferyl acetate (ACC) substrate at room temperature for 9 min in a total volume of 50 μL. Dimethyl sulfoxide (10% v/v) was included to dissolve the substrate. For the steady-state initial velocity kinetics the substrate concentrations were varied from 0.01 to 5 mM. The sample was excited at 386 nm and continuously monitored for the increase in fluorescence emission at 446 nm. The production of phenol was quantified using 7 hydroxycoumarin-4-carboxylic acid as a standard. The fluorescence intensity data were analyzed as above by using nonlinear regression analysis with Grafit.[28] All measurements were performed in triplicate.

pH Dependence of IcaB. The pH dependence of the enzyme reaction was measured between pH 5.0 and 9.0 at 37 °C using the fluorescamine assay described above with a PNAG oligomer mixture of tetramer and pentamer GlcNAc using a 100 mM phosphate buffer system (37 °C) containing 250 mM NaCl. The substrate and the enzyme concentrations in the assay were as follows: 10 μM $IcaB_{His10}$, 10 μM of $CoCl_2$, 50 mM substrate.

PNAG Oligomer Length Dependent IcaB Activity. The GlcNAc length dependence of $IcaB_{His10}$ was measured using the fluorescamine assay described above with the following substrates: *N*-acetylglucosamine, $(GlcNAc)_2$, $(GlcNAc)_3$, $(GlcNAc)_4$, $(GlcNAc)_5$, and $(GlcNAc)_6$. The oligosaccharide concentrations were determined using ^1H NMR and DMF as an internal standard. The samples contained 30 μM $IcaB_{His10}$, 30 μM $CoCl_2$, and 50 mM substrate.

Metal Dependent Activity. The enzyme (30 μM) in buffer B was preincubated in the presence of various divalent metals as chloride or sulfate salt solutions (30 μM) or metal chelators (1 mM) at room temperature for 30 min. The mixture was then incubated at 37 °C for 24 h with 50 mM of the PNAG GlcNAc tetramer and pentamer oligomer mixture, and the amount of de-*N*-acetylation quantified using the fluorescamine assay described above. All Fe(II) assay steps were performed in a glovebox with degassed buffers for the Fe(II) salt until the end of the incubation.

To analyze metal dependence of the apo-IcaB, the purified protein (30 μM) was incubated with 3 mM dipicolinic acid (DPA) for 1 h at room temperature in buffer B. The protein solution was then desalted with a PD-10 column pre-equilibrated with Chelex treated buffer B. The fractions were concentrated with a 10 000 MWCO centrifugal filter. The apoenzyme (20 μM) in buffer B was preincubated in the presence of various divalent metals as chloride or sulfate salt solutions (20 μM) at room temperature for 30 min. The mixture was then incubated at 37 °C for 24 h with 50 mM PNAG GlcNAc tetramer−pentamer oligomer mixture. The activity of the enzyme was measured in triplicate using the fluorescamine assay described above. The assays with Fe(II) were carried out anaerobically in a glovebox as described above.

Metal Analysis. Inductively coupled plasma−atomic emission spectroscopy (ICP-AES) was carried out at the Analytical Lab for Environmental Research and Training at the University of Toronto. ICP-AES samples were prepared by diluting concentrated enzyme samples to 5 μM in 5 mM phosphate buffer, pH 7.5. Control samples were prepared using 5 mM phosphate buffer, pH 7.5, and were subtracted from the signals acquired from the enzyme samples during ICP-AES analysis.

Determination of the De-*N*-acetylation Position by IcaB on PNAG Oligomers. The position of de-*N*-acetylation within the PNAG oligomers was determined by using ESI-MS/MS analysis. GlcNAc oligomers (50 mM) were incubated with $IcaB_{His10}$ (100 μM) in buffer B with 1 mg/mL bovine serum albumin (BSA) for 48 h at 37 °C in a total volume of 100 μL. The mixture was then diluted to 1.5 mL and dialyzed against deionized water by using a 100 MWCO membrane (Spectrapor). The resulting mixture was lyophilized and redissolved in 500 μL of deionized water. To separate deacetylated PNAG oligomer from the non-deacetylated material, the samples were purified on a small (~500 μL) Dowex 50Wx2-100 column equilibrated with deionized water. The sample solution was loaded onto the column, and the column was washed with 3 mL of deionized water. The de-*N*-acetylated products were eluted with 1.5 mL 10% (v/v) NH_4OH and lyophilized. The resulting solid was redissolved in deionized water (100 μL) and analyzed by ESI-MS/MS.

To simplify the fragment deconvolution of de-*N*-acetylated GlcNAc pentamer and hexamer, the reducing end of the oligosaccharides was reduced prior to ion exchange purification. The enzyme reaction was diluted to 1 mL with water and treated with sodium borohydride (1−3 mg) for 12 h at room temperature. The reaction was quenched with acetic acid (~20 μL) and treated as described above.

Tandem MS was performed on the samples in positive mode using an AB Sciex QSTAR instrument with a TurboIonSpray source.

RESULTS

Overexpression and Purification of Recombinant IcaB. Residues (30−289) of *S. epidermidis* IcaB were expressed in *E. coli* from a pET16b plasmid to give $IcaB_{His10}$, which lacked the native N-terminal signal peptide and carried an N-terminal ten histidine tag. To minimize the formation of inclusion bodies, protein expression was induced at 10 °C with IPTG. Homogenous protein ($IcaB_{His10}$), as judged by Coomassie stained SDS-PAGE analysis, was achieved after purification on a Ni(II)-NTA column (Figure S1A). It was necessary to maintain a high ionic strength in all buffers (>500 mM NaCl) to prevent protein aggregation and precipitation. After dialysis the protein was supplemented with 5% (v/v) glycerol and could be stored at 4 °C for up to 10 days with no significant loss of activity. The typical yield of purified enzyme was ~5 mg/L. Gel filtration analysis showed one predominant species with apparent molecular mass of 33 kDa, suggesting that the protein is monomeric at the concentrations evaluated (Figure S2). The calculated molecular mass of the recombinant His-tagged protein (33 113 Da) was confirmed by ESI-MS (data not shown). The His-tag could be cleaved from the construct with FactorXa protease to yield IcaB (Figure S1B).

dx.doi.org/10.1021/bi400836g | *Biochemistry* 2013, 52, 5463−5471

Activity of IcaB. Previous studies have shown deletion mutants of IcaB in *S. epidermidis* result in the formation of fully acetylated PNAG, suggesting that IcaB is responsible for PNAG de-*N*-acetylation.[21] To assess IcaB's de-*N*-acetylase activity *in vitro* recombinant $IcaB_{His10}$ was incubated with synthetic PNAG oligomers and de-*N*-acetylation was monitored using a fluorescamine assay.[29] Time dependent de-*N*-acetylation of the PNAG oligomers was observed (data not shown). No de-*N*-acetylation activity was observed against chitotetraose (β-1,4-linked GlcNAc) under similar conditions, suggesting IcaB has specificity for PNAG de-*N*-acetylation (data not shown).

Using the fluorescamine assay with the oligomeric PNAG substrates, the metal and pH dependence of IcaB activity was evaluated. The pH dependence of $IcaB_{His10}$ was consistent with observations for other CE4 members showing increasing de-*N*-acetylase activity with pH up to approximately pH 8 (Figure 2).[26] Incubation of IcaB or $IcaB_{His10}$ with metal chelators (EDTA or DPA) dramatically reduced the de-*N*-acetylase activity, supporting the metal dependence of the enzyme (Figure 3). Analysis of the as-isolated protein by ICP-AES showed the predominant metal copurifying with the enzyme to be zinc although nickel, manganese, calcium, and magnesium were also present (data not shown). The addition of divalent metals to as isolated $IcaB_{His10}$ or IcaB did not provide substantial increases in de-*N*-acetylation activity, with the exception of Co^{2+}, which gave a 4-fold increase over the as isolated protein (Figure 3). Significant decreases in activity were observed for Ni^{2+}, Mn^{2+}, and Fe^{2+} for $IcaB_{His10}$ but not IcaB, suggesting metal chelation to the His-tag effects de-*N*-acetylation activity. Apo-IcaB was isolated by incubation with the chelator DPA followed by size exclusion chromatography. The isolated apoenzyme, in the absence of metal chelator, retained approximately 15% of the activity of the as isolated enzyme, likely due to low level divalent metal contamination (Figure 4). Addition of stoichiometric metal to the apoenzyme resulted in the recovery of activity with the highest activity observed for Co^{2+}, Zn^{2+}, and Mn^{2+} (Figure 4). The metal loading of the enzyme was confirmed by ICP-AES analysis,

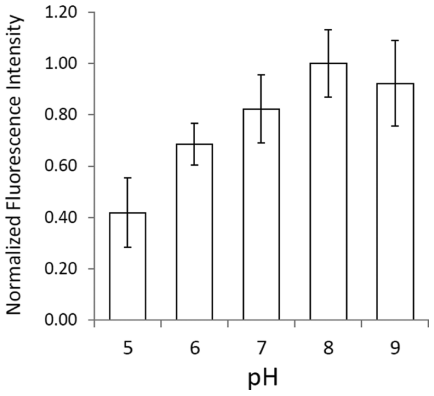

Figure 2. pH activity profile of IcaB. $IcaB_{His10}$ (10 μM), $CoCl_2$ (10 μM), and PNAG substrate (50 mM mixture of tetramer and pentamer) were incubated 24 h in an sodium phosphate buffer (100 mM with 250 mM NaCl). The amount of de-*N*-acetylation was determined using a fluorescamine assay. Bars represent standard deviation of triplicate experiments.

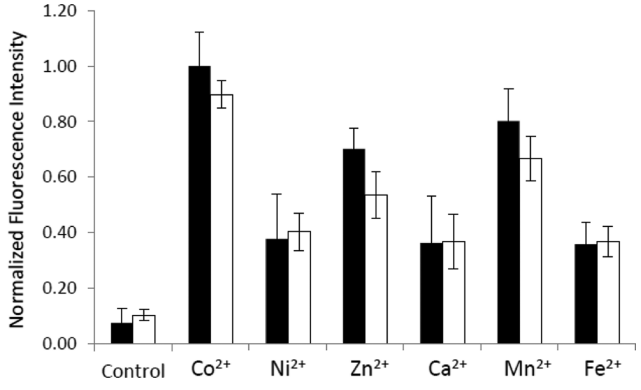

Figure 4. Metal dependent activity of apo-IcaB. Apo-protein (20 μM) was incubated at 37 °C for 24 h with PNAG substrate (50 mM mixture of tetramer and pentamer) and metal ion (20 μM) in buffer B. Control is DPA treated apo-protein prior to additional metal ions. All metals were added as chloride or sulfate salts. $IcaB_{His10}$ (black) or IcaB (white). Bars represent standard deviation of triplicate experiments.

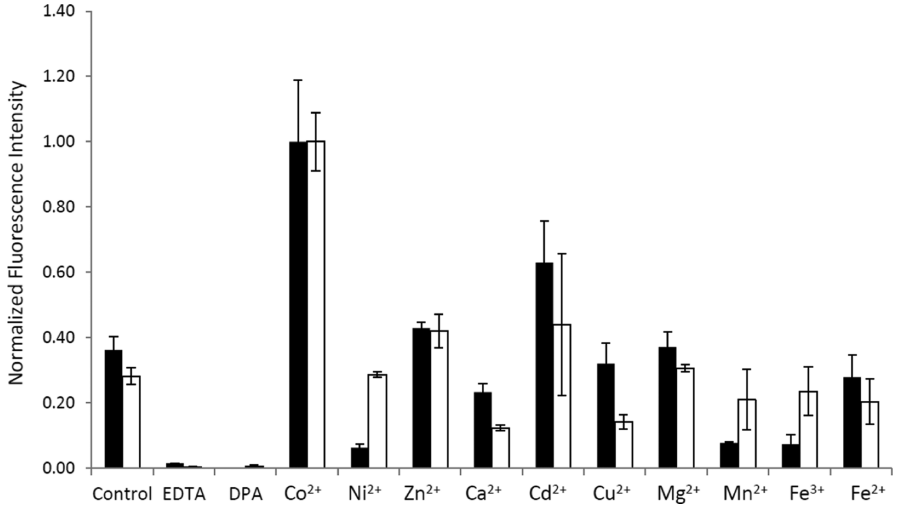

Figure 3. Metal dependence of IcaB activity. $IcaB_{His10}$ (30 μM) was incubated at 37 °C for 24 h with PNAG substrate (50 mM mixture of tetramer and pentamer) and either metal ion (30 μM) or metal chelator (1 mM) in buffer B. All metals were added as chloride or sulfate salts. Control is purified as isolated $IcaB_{His10}$ (black) or IcaB (white). Bars represent standard deviation of triplicate experiments.

dx.doi.org/10.1021/bi400836g | *Biochemistry* 2013, 52, 5463−5471

where enzyme incubated with Zn^{2+} or Co^{2+} showed 80% and 50% metal loading, respectively, after extensive dialysis (data not shown).

As an alternative to the fluorescamine end point assay it was found that IcaB also hydrolyzes the fluorogenic substrate 3-carboxyumberlliferyl acetate (ACC).[27] This ester provides a useful substrate for comparison to other CE4 enzymes, which recognize other saccharide amide or ester substrates. Similar patterns of metal dependent activity were observed for the enzyme with ACC, suggesting a similar mechanism for ester cleavage (data not shown).

De-*N*-acetylation of PNAG Oligomers. dPNAG isolated from *S. epidermidis* on average contains one de-*N*-acetylation every 4−5 GlcNAc residues.[7] Digestion analysis of isolated dPNAG has found no defined pattern of de-*N*-acetylation along the polymer, and there are likely spans of low de-*N*-acetylation as well as regions of higher de-*N*-acetylation.[7] Despite no defined pattern of de-*N*-acetylation being observed in the global analysis of the dPNAG polymer, the de-*N*-acetylation positions may be biased by the substrate recognition of IcaB influencing the local de-*N*-acetylation positions in the polymer. To evaluate the size of the PNAG polymer recognized at the IcaB active site, the length dependence of the de-*N*-acetylation activity was evaluated with a panel of synthetic oligomeric PNAG substrates.[25] It was necessary to carefully standardize the oligomer concentrations using ^{1}H NMR as the oligomer samples contained varying amounts of water after lyophilization. Using the fluorescamine assay, the PNAG oligomers were incubated with $IcaB_{His10}$ and the extent of de-*N*-acetylation was evaluated (Figure 5). No de-*N*-acetylation activity was observed

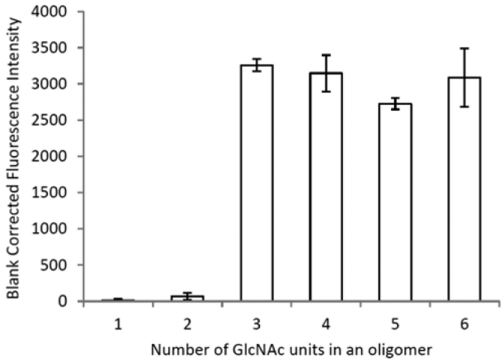

Figure 5. Substrate length dependence of IcaB. PNAG oligomers (50 mM) of varying length were incubated with $IcaB_{His10}$ (30 μM) and $CoCl_2$ (30 μM) in buffer B. Substrate concentrations were standardized using ^{1}H NMR. Amount of de-*N*-acetylation was determined using the fluorescamine assay. Bars represent standard deviation of triplicate experiments.

with the mono- or disaccharide substrates, while longer oligomers from trisaccharide up to a hexasaccharide showed equivalent levels of de-*N*-acetylation. These results suggest that the occupancy of a minimum of two subsites in addition to the active site are required for productive de-*N*-acetylation.

To further refine the model of IcaB activity, the position of de-*N*-acetylation within PNAG oligomers were determined by ESI MS/MS analysis (Figure 6 and Figures S3−S5). Because of the low catalytic activity of IcaB (see below), only small a small fraction of the oligomers were de-*N*-acetylated. Thus, it was necessary to separate the non-de-*N*-acetylated oligomers from the products of the reaction using cation exchange chromatography prior to analysis. Regardless of the oligomer length only mono-de-*N*-acetylated products were observed. The mono-de-*N*-acetylated tri- and tetrasaccharide substrates (ions of m/z 586.3 or 789.3, respectively) were fragmented to give masses consistent with de-*N*-acetylation at all possible positions within the oligomers (Figures S3 and S4). In order to simplify the analysis of the de-*N*-acetylated penta- and hexasaccharide substrates, the oligosaccharides were reduced prior to analysis with sodium borohydride. The ions that correspond to mono-de-*N*-acetylated products of the penta- and hexasaccharide were fragmented (ions of m/z 994.4 or 1097.5, respectively) (Figure 6 and Figure S5). Interestingly, it was found that PNAG pentasaccharide was de-*N*-acetylated only at the second GlcNAc residue from the reducing terminus (Figure 6A). MS/MS analysis of the partially de-*N*-acetylated PNAG hexasaccharide gave two main de-*N*-acetylation positions at the second and third GlcNAc residues from the reducing terminus (Figure 6B and Figure S5). These results are counterintuitive given the similar levels of de-*N*-acetylation activity across the tri- through hexasaccharide substrates (Figure 5). IcaB may have an extended active site, which recognizes the larger oligomers but contributes no net difference toward the overall de-*N*-acetylation catalysis beyond a trisaccharide.

Given the similar levels of de-*N*-acetylation observed for the tri- through hexasaccharide PNAG oligomers and differences in regiochemistry of de-*N*-acetylation observed with the oligomers, the tri- and pentasaccharide substrates were subjected to further kinetic analysis. Following the de-*N*-acetylation of the oligomers with 6 time points over 24 h showed a linear increase in de-*N*-acetylation while the total amount of de-*N*-acetylation remained under 1%. The initial velocity was determined at substrate concentrations from 10 to 200 mM, and the Michaelis−Menten parameters were calculated by direct curve fitting (Figure 7). The values obtained for the trisaccharide and pentasaccharide were the same within experimental error, consistent with the substrate length de-*N*-acetylation dependence described above.

DISCUSSION

The importance of IcaB in dPNAG dependent biofilm formation makes it an attractive target for the design of inhibitors targeting *Staphylococcal* biofilms. Recent structural and functional characterization of the IcaB homologue from *E. coli,* PgaB, provides perspective on the differences between these important de-*N*-acetylases in Gram-positive and Gram-negative systems. Although these proteins perform the same reaction, the proteins differ in both size and cellular localization. PgaB is a two-domain periplasmic lipoprotein, with an N-terminal de-*N*-acetylase domain and a C-terminal domain that is proposed to be a carbohydrate-binding domain. IcaB is homologous to the *N*-terminal domain of PgaB (24% identity and 55% similarity). IcaB was found to have a low catalytic efficiency (k_{cat}/K_M 0.03 M^{-1} s^{-1} for PNAG pentamer) against the synthetic oligomers consistent with our previous kinetic analysis of PgaB (k_{cat}/K_M 0.26 M^{-1} s^{-1} against the PNAG pentamer). These catalytic parameters are poor in comparison with the majority of other characterized enzymes which on average have k_{cat} (s^{-1}) values greater that unity and k_{cat}/K_M values greater that 10^4 (M^{-1} s^{-1}).[30] Other CE4 de-*N*-acetylases are also considerably better catalysts (e.g., *Streptococcus pneumoniae* peptidoglycan de-*N*-acetylase (*Sp*PgdA) k_{cat} 0.6 s^{-1}, k_{cat}/K_M 150 M^{-1} s^{-1} against chitotriose) than the PNAG

dx.doi.org/10.1021/bi400836g | *Biochemistry* 2013, 52, 5463−5471

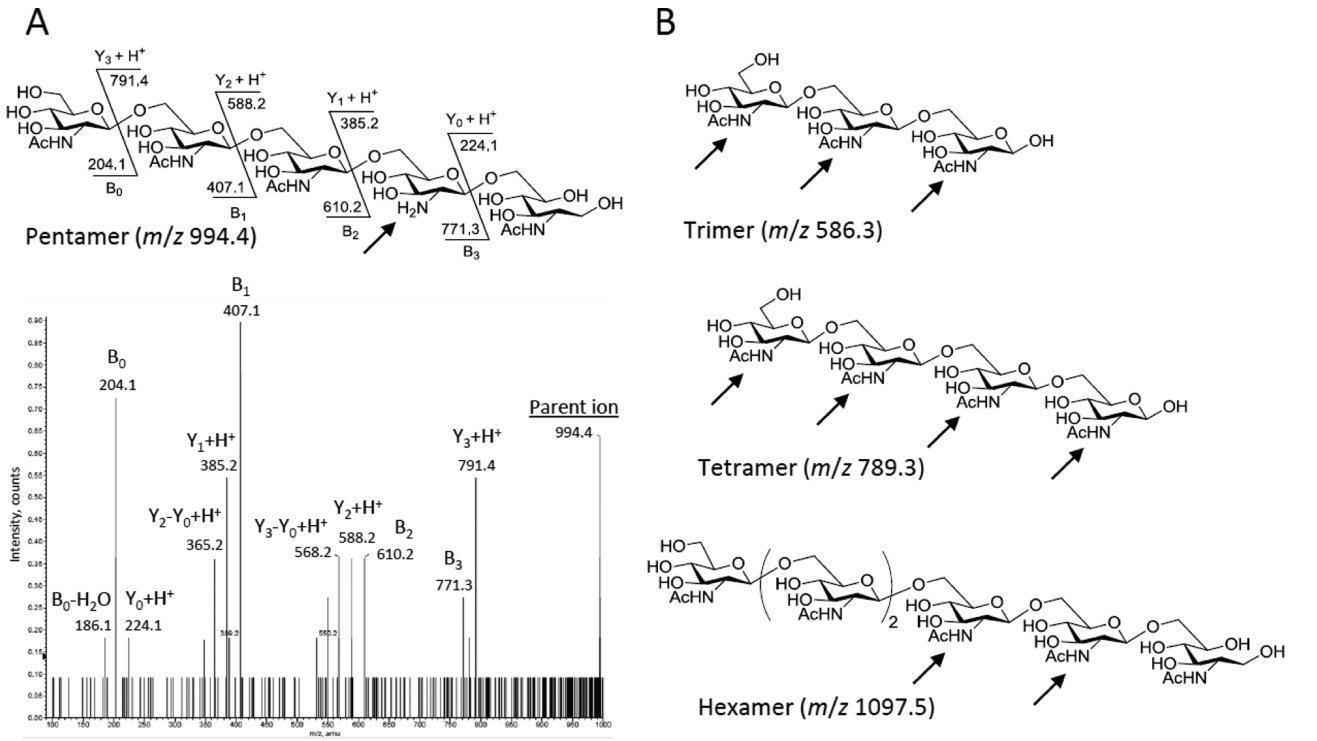

Figure 6. (A). Structure and calculated molecular weights of each fragment of mono-de-*N*-acetylated GlcNAc pentasaccharide observed in tandem ESI-MS/MS analysis. (B) Structures of GlcNAc oligomers analyzed with the sites of deacetylation shown with arrows.

de-*N*-acetylases IcaB and PgaB.[26] However, when IcaB's kinetic parameters (k_{cat} 0.0007 s^{-1}) are compared with other enzymes that act on biofilm matrix polysaccharides such as the alginate epimerase AlgG ($k_{cat} \sim 0.02\ s^{-1}$), the parameters are more consistent.[31] The low catalytic proficiencies of these biofilm matrix enzymes may be related to the slowed metabolic activity and the extended doubling times of bacteria residing in biofilms and the incomplete de-*N*-acetylation or epimerization found on these biofilm matrix polysaccharides. Also, given the extracellular nature of IcaB, the enzyme likely has extended exposure to the PNAG polymer substrate in comparison with PgaB and AlgG which act as the polysaccharide transits the periplasm; thus, the extended exposure time to the polysaccharide substrate would require further reductions in catalytic activity to maintain low levels (~20%) of PNAG de-*N*-acetylation observed.

The poor activity of PgaB in comparison with other CE4 de-*N*-acetylases was rationalized based on the structure of the active site, which showed the absence of a key Asp residue.[23] In the *Sp*PgdA Asp391 is hydrogen bonded to the catalytic His417 residue (Figure 8C). His417 is proposed to protonate the tetrahedral intermediate leading to amide bond hydrolysis.[26] We have hypothesized that the lack of this important acidic residue in the PgaB de-*N*-acetylase active site attenuates the enzyme's activity.[23] Homology models of IcaB were built using Phyre[2] to evaluate the similarity of IcaB to PgaB and other structurally characterized CE4 de-*N*-acetylases.[32] The best models generated were based on the structures of PgaB (PDB: 4F9D) as well as the putative polysaccharide deacetylase bc0361 (PDB: 4HD5) from *Bacillus cereus* with alignment coverage over 90% of the IcaB sequence.[23,33] Both of these models indicate that the catalytic His47 residue of IcaB does not have an acidic hydrogen-bonding partner, suggesting IcaB's activity may be attenuated for similar reasons to PgaB (Figure 8A,B). Overlays of the active site of IcaB and the highly active CE4 de-*N*-acetylase *Sp*PgdA show the conservation of the other active site residues (Figure 8C).

In contrast to previous studies on PgaB, it was possible to saturate the activity of IcaB with the PNAG oligomers allowing calculation of the Michaelis–Menten parameters. The K_M (20–30 mM) of IcaB for the oligomeric substrates is significantly lower than the K_M of PgaB (>50 mM) which could only be estimated as the enzyme activity was not saturated at the solubility limit of the PNAG oligomers. One explanation for this difference is that IcaB lacks the putative carbohydrate binding domain present in PgaB, and thus the active site of IcaB requires higher substrate affinity. In PgaB the full length PNAG substrate may span the domains allowing the C-terminal domain to provide affinity for the polymer; the PNAG oligomers assayed are not of sufficient length to span the domains. From the models of IcaB it is evident that PgaB has two extended loops that lie on one side of the active site, which are absent in IcaB (Figure 8). These differences in structure flanking the active site are consistent with different recognition in the binding subsites that result in altered positional preferences for de-*N*-acetylation and the differential dependence on oligomer length observed between the two enzymes with the PNAG oligomers. It is important to note that the PgaB active site is also found in close proximity to the C-terminal domain which may contribute to substrate recognition. One model of substrate recognition consistent with the data would be dominant recognition by IcaB of the nonreducing terminal portion of the polymer by the region flanking the active site that lacks homology to PgaB. This would explain the preference for de-*N*-acetylation close to the reducing terminus of the larger oligomers by IcaB as well as the IcaB's lower K_M in comparison with PgaB. As PgaB is found to preferentially de-*N*-acetylate the central residue in a PNAG pentasaccharide and have a weaker

dx.doi.org/10.1021/bi400836g | *Biochemistry* 2013, 52, 5463–5471

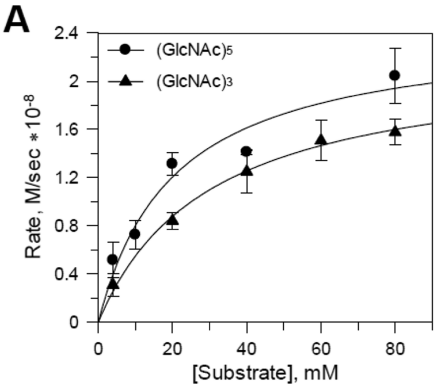

	K_M (mM)	V_{max} (M sec^{-1} 10^{-8})	k_{cat} (s^{-1} 10^{-3})	k_{cat}/K_M (M^{-1} s^{-1})
$(GlcNAc)_3$	30 ± 4	2 ± 0.1	0.7 ± 0.03	0.02
$(GlcNAc)_5$	20 ± 6	2 ± 0.2	0.7 ± 0.06	0.03
ACC	0.5 ± 0.1	4 ± 0.2	1.3 ± 0.1	2.5

Figure 7. Steady-state kinetics for $IcaB_{His10}$ using (A) PNAG $(GlcNAc)_3$ and $(GlcNAc)_5$ or (B) ACC as substrates. Initial velocities were calculated after 10 h ($(GlcNAc)_3$ or $(GlcNAc)_5$) or 9 min (ACC) of incubation with 30 μM $IcaB_{His10}$ and 30 μM $CoCl_2$ in buffer B at indicated substrate concentrations.

oligomer affinity, the subsite binding energy must be more evenly distributed across the reducing and nonreducing terminal subsites.

Using an unnatural coumarin-based fluorogenic substrate ACC, it is possible to compare the k_{cat} parameters of PgaB (0.013 s^{-1}) and IcaB (0.0007 s^{-1}) as the K_M values of this substrate can be determined for both enzymes.[27] These values are consistent with the differences in k_{cat}/K_M seen with the oligomeric PNAG substrates. The k_{cat} values of the ester and natural amide substrates for IcaB are similar (0.0013 vs 0.0007 s^{-1}). This is counterintuitive given the electronic differences between esters and amides, but similar observations have been made with other metaloamidases.[34] The activity of *Sp*PgdA with a similar unnatural substrate to ACC, 4-methylumbelliferyl acetate, shows 1000−10 000 times higher k_{cat} and k_{cat}/K_M values, further emphasizing the attenuated catalysis of PNAG de-*N*-acetylases for not only unnatural but also the native substrate.[35]

The metal dependence of IcaB was analyzed with and without the N-terminal His tag. The activity of the as-isolated enzyme was not dramatically affected by the addition of divalent metals, suggesting the recombinant IcaB consistently copurified with metal cofactors, predominately zinc (data not shown). Addition of divalent metals to apo-IcaB gave similar increases across a range of divalent metals with the highest activity being observed with Co^{2+}. Optimal deacetylase activity is often observed with Co^{2+} in CE4 enzymes, although it is unlikely to be the naturally occurring cofactor due to its low bioavailability.[23,26,36−38] Interestingly, in contrast to the observations for PgaB, significant increases in activity, above other divalent ions, was not observed on addition Ni^{2+} or Fe^{2+}, but a general increase in activity was observed with all the divalent metal ions evaluated (Figure 4).[20] The promiscuous metal dependence of IcaB suggests the enzyme can use a variety of metals depending on their availability. This is consistent with IcaB being an extracellular protein that can use the divalent metal available in a range of environmental conditions.

In conclusion, we have demonstrated that IcaB exhibits de-*N*-acetylase activity on PNAG oligomers. IcaB has poor catalytic activity consistent with the results observed for its *E. coli* homologue, PgaB, as well as the alginate epimerase AlgG, suggesting this may be a common feature of enzymes that act on biofilm matrix polysaccharides.[23,31] The observed substrate recognition and metal dependence of the enzyme will facilitate the design of biofilm inhibitors targeting IcaB.

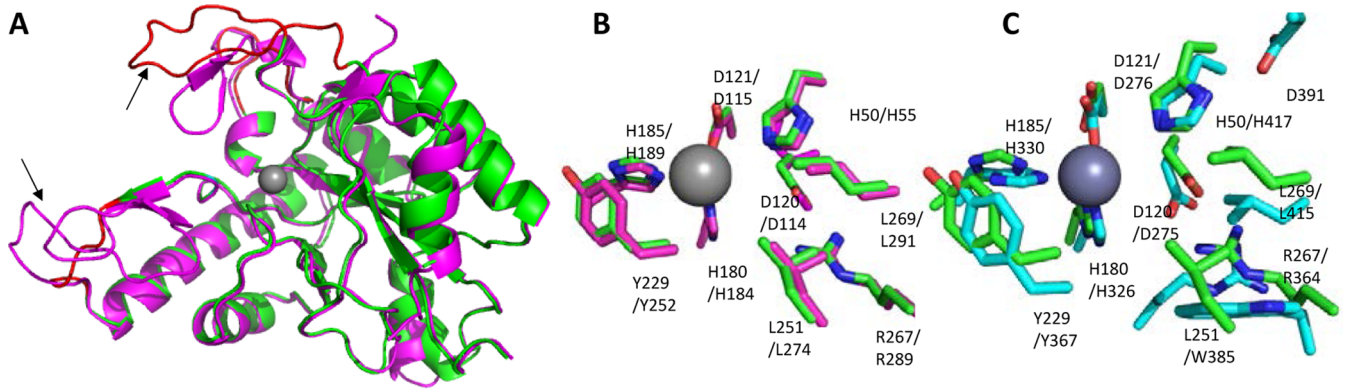

Figure 8. Structural comparison of the Phyre[2] generated model of IcaB and *E. coli* PgaB and *Sp*PgdA. (A) Cartoon representation of the IcaB model (green) and its superposition with the N-terminal domain of PgaB (PDB: 4F9D, magenta). Black arrows indicate loops with substantial predicted structural differences. Superposition of the active site residues of (B) IcaB (green) and PgaB (magenta) and (C) IcaB and *Sp*PgdA. In all panels the active site metal ion is shown as a gray sphere.

dx.doi.org/10.1021/bi400836g | *Biochemistry* 2013, 52, 5463−5471

■ ASSOCIATED CONTENT

Supporting Information

$IcaB_{His10}$ expression and purification SDS-PAGE gel, gel filtration chromatography of $IcaB_{His10}$ and IcaB, ESI-MS/MS analysis of the $[M + H]^+$ precursor ion, structures and calculated molecular weights of each fragment of monode-*N*-acetylated GlcNAc trisaccharides, tetrasaccharides, and hexasaccharides. This material is available free of charge via the Internet at http://pubs.acs.org.

■ AUTHOR INFORMATION

Corresponding Author

*E-mail mnitz@chem.utoronto.ca, phone 416-946-0640 (M.N.).

Funding

This work is supported in part by research grants from the Canadian Institutes of Health Research (CIHR) #43998 to P.L.H. and #89708 to M.N. D.J.L. was supported, in part, by graduate scholarships from the University of Toronto, the Ontario Graduate Scholarship program, and CIHR. P.L.H. is the recipient of a Canada Research Chair.

Notes

The authors declare no competing financial interest.

■ ACKNOWLEDGMENTS

We thank Deborah Zamble and Michael Otto for helpful discussions.

■ ABBREVIATIONS

PNAG, β-1,6-linked *N*-acetylglucosamine; dPNAG, de-*N*-acetylated β-1,6-linked *N*-acetylglucosamine; PIA, polysaccharide intercellular adhesin; CE4, family 4 carbohydrate esterases; UDP, uridine diphosphate; GlcNAc, *N*-acetylglusamine; CAZy, carbohydrate-active enzymes; NTA, Ni(II)-nitrilotriacetic acid; SDS-PAGE, sodium dodecyl sulfate−polyacrylamide gel electrophoresis; ESI-MS, electrospray ionization mass spectrometry; EDTA, ethylenediaminetetraacetic acid; BCA, bicinchoninic acid; MALDI-MS, matrix-assisted laser desorption/ionization mass spectrometry; DMF, dimethylformamide; ACC, 3-carboxyumberlliferyl acetate; DPA, dipicolinic acid; (ICP-AES), inductively coupled plasma−atomic emission spectroscopy.

■ REFERENCES

(1) Joo, H. S., and Otto, M. (2012) Molecular basis of in vivo biofilm formation by bacterial pathogens. *Chem. Biol. 19*, 1503−1513.

(2) Costerton, J. W., Stewart, P. S., and Greenberg, E. P. (1999) Bacterial biofilms: a common cause of persistent infections. *Science 284*, 1318−1322.

(3) Donlan, R. M., and Costerton, J. W. (2002) Biofilms: survival mechanisms of clinically relevant microorganisms. *Clin. Microbiol. Rev. 15*, 167−193.

(4) Potera, C. (1999) Microbiology - Forging a link between biofilms and disease. *Science 283*, 1837−1839.

(5) Vu, B., Chen, M., Crawford, R. J., and Ivanova, E. P. (2009) Bacterial extracellular polysaccharides involved in biofilm formation. *Molecules 14*, 2535−2554.

(6) Zhao, K., Tseng, B. S., Beckerman, B., Jin, F., Gibiansky, M. L., Harrison, J. J., Luijten, E., Parsek, M. R., and Wong, G. C. (2013) Psl trails guide exploration and microcolony formation in Pseudomonas aeruginosa biofilms. *Nature 497*, 388−391.

(7) Mack, D., Fischer, W., Krokotsch, A., Leopold, K., Hartmann, R., Egge, H., and Laufs, R. (1996) The intercellular adhesin involved in biofilm accumulation of Staphylococcus epidermidis is a linear beta-1,6-linked glucosaminoglycan: Purification and structural analysis. *J. Bacteriol. 178*, 175−183.

(8) Cerca, N., Jefferson, K. K., Maira-Litran, T., Pier, D. B., Kelly-Quintos, C., Goldmann, D. A., Azeredo, J., and Pier, G. B. (2007) Molecular basis for preferential protective efficacy of antibodies directed to the poorly acetylated form of staphylococcal poly-N-acetyl-beta-(1−6)-glucosaminev. *Infect. Immun. 75*, 3406−3413.

(9) Wang, X., Preston, J. F., and Romeo, T. (2004) The pgaABCD locus of Escherichia coli promotes the synthesis of a polysaccharide adhesin required for biofilm formation. *J. Bacteriol. 186*, 2724−2734.

(10) Choi, A. H., Slamti, L., Avci, F. Y., Pier, G. B., and Maira-Litran, T. (2009) The pgaABCD locus of Acinetobacter baumannii encodes the production of poly-beta-1,6-N-acetylglucosamine, which is critical for biofilm formation. *J. Bacteriol. 191*, 5953−5963.

(11) Sloan, G. P., Love, C. F., Sukurnar, N., Mishra, M., and Deora, R. (2007) The Bordetella Bps polysaccharide is critical for biofilm development in the mouse respiratory tract. *J. Bacteriol. 189*, 8270−8276.

(12) Conover, M. S., Sloan, G. P., Love, C. F., Sukumar, N., and Deora, R. (2010) The Bps polysaccharide of Bordetella pertussis promotes colonization and biofilm formation in the nose by functioning as an adhesin. *Mol. Microbiol. 77*, 1439−1455.

(13) Izano, E. A., Sadovskaya, I., Vinogradov, E., Mulks, M. H., Velllyagounder, K., Ragunath, C., Kher, W. B., Ramasubbu, N., Jabbouri, S., Perry, M. B., and Kaplan, J. B. (2007) Poly-N-acetylglucosamine mediates biofilm formation and antibiotic resistance in Actinobacillus pleuropneumoniae. *Microb. Pathog. 43*, 1−9.

(14) Yakandawala, N., Gawande, P. V., LoVetri, K., Cardona, S. T., Romeo, T., Nitz, M., and Madhyastha, S. (2011) Characterization of the poly-beta-1,6-N-acetylglucosamine polysaccharide component of Burkholderia biofilms. *Appl. Environ. Microbiol. 77*, 8303−8309.

(15) Itoh, Y., Wang, X., Hinnebusch, B. J., Preston, J. F., and Romeo, T. (2005) Depolymerization of beta-1,6-N-acetyl-D-glucosamine disrupts the integrity of diverse bacterial biofilms. *J. Bacteriol. 187*, 382−387.

(16) Otto, M. (2008) Staphylococcal biofilms. *Curr. Top. Microbiol. Immunol. 322*, 207−28.

(17) Heilmann, C., Schweitzer, O., Gerke, C., Vanittanakom, N., Mack, D., and Gotz, F. (1996) Molecular basis of intercellular adhesion in the biofilm-forming Staphylococcus epidermidis. *Mol. Microbiol. 20*, 1083−1091.

(18) Heilmann, C., and Gotz, F. (1998) Further characterization of Staphylococcus epidermidis transposon mutants deficient in primary attachment or intercellular adhesion. *Zentralbl. Bakteriol. 287*, 69−83.

(19) Heilmann, C., Gerke, C., Perdreau-Remington, F., and Gotz, F. (1996) Characterization of Tn917 insertion mutants of Staphylococcus epidermidis affected in biofilm formation. *Infect. Immun. 64*, 277−282.

(20) Gerke, C., Kraft, A., Sussmuth, R., Schweitzer, O., and Gotz, F. (1998) Characterization of the N-acetylglucosaminyltransferase activity involved in the biosynthesis of the Staphylococcus epidermidis polysaccharide intercellular adhesin. *J. Biol. Chem. 273*, 18586−18593.

(21) Vuong, C., Kocianova, S., Voyich, J. M., Yao, Y. F., Fischer, E. R., DeLeo, F. R., and Otto, M. (2004) A crucial role for exopolysaccharide modification in bacterial biofilm formation, immune evasion, and virulence. *J. Biol. Chem. 279*, 54881−54886.

(22) Cantarel, B. L., Coutinho, P. M., Rancurel, C., Bernard, T., Lombard, V., and Henrissat, B. (2009) The Carbohydrate-active EnZymes database (CAZy): an expert resource for Glycogenomics. *Nucleic Acids Res. 37*, D233−D238.

(23) Little, D. J., Poloczek, J., Whitney, J. C., Robinson, H., Nitz, M., and Howell, P. L. (2012) The structure- and metal-dependent activity of Escherichia coli PgaB provides insight into the partial de-N-acetylation of poly-beta-1,6-N-acetyl-D-glucosamine. *J. Biol. Chem. 287*, 31126−31137.

(24) Nishiyama, T., Noguchi, H., Yoshida, H., Park, S. Y., and Tame, J. R. (2013) The structure of the deacetylase domain of Escherichia coli PgaB, an enzyme required for biofilm formation: a circularly

permuted member of the carbohydrate esterase 4 family. *Acta Crystallogr., Sect. D: Biol. Crystallogr. 69*, 44−51.
(25) Leung, C., Chibba, A., Gomez-Biagi, R. F., and Nitz, M. (2009) Efficient synthesis and protein conjugation of beta-(1→6)-D-N-acetylglucosamine oligosaccharides from the polysaccharide intercellular adhesin. *Carbohydr. Res. 344*, 570−575.
(26) Blair, D. E., Schuttelkopf, A. W., MacRae, J. I., and van Aalten, D. M. F. (2005) Structure and metal-dependent mechanism of peptidoglycan deacetylase, a streptococcal virulence factor. *Proc. Natl. Acad. Sci. U. S. A. 102*, 15429−15434.
(27) Chibba, A., Poloczek, J., Little, D. J., Howell, P. L., and Nitz, M. (2012) Synthesis and evaluation of inhibitors of E. coli PgaB, a polysaccharide de-N-acetylase involved in biofilm formation. *Org. Biomol. Chem. 10*, 7103−7107.
(28) Leatherbarrow, R. J. (2011) GraFit Version 7, Erithacus Software Limited, London, UK.
(29) Udenfriend, S., Stein, S., Bohlen, P., Dairman, W., Leimgruber, W., and Weigele, M. (1972) Fluorescamine: a reagent for assay of amino acids, peptides, proteins, and primary amines in the picomole range. *Science 178*, 871−872.
(30) Bar-Even, A., Noor, E., Savir, Y., Liebermeister, W., Davidi, D., Tawfik, D. S., and Milo, R. (2011) The moderately efficient enzyme: evolutionary and physicochemical trends shaping enzyme parameters. *Biochemistry 50*, 4402−4410.
(31) Jerga, A., Raychaudhuri, A., and Tipton, P. A. (2006) Pseudomonas aeruginosa C5-mannuronan epimerase: steady-state kinetics and characterization of the product. *Biochemistry 45*, 552−560.
(32) Kelley, L. A., and Sternberg, M. J. (2009) Protein structure prediction on the Web: a case study using the Phyre server. *Nat. Protoc. 4*, 363−371.
(33) Fadouloglou, V. E., Kapanidou, M., Agiomirgianaki, A., Arnaouteli, S., Bouriotis, V., Glykos, N. M., and Kokkinidis, M. (2013) Structure determination through homology modelling and torsion-angle simulated annealing: application to a polysaccharide deacetylase from Bacillus cereus. *Acta Crystallogr., Sect. D: Biol. Crystallogr. 69*, 276−283.
(34) Suh, J. H., Park, T. H., and Hwang, B. K. (1992) Comparable rates for cleavage of amide and ester bonds through nucleophilic-attack by carboxylate anion and general acid catalysis by metal-bound water in a carboxypeptidase-a model. *J. Am. Chem. Soc. 114*, 5141−5146.
(35) Bui, N. K., Turk, S., Buckenmaier, S., Stevenson-Jones, F., Zeuch, B., Gobec, S., and Vollmer, W. (2011) Development of screening assays and discovery of initial inhibitors of pneumococcal peptidoglycan deacetylase PgdA. *Biochem. Pharmacol. 82*, 43−52.
(36) Deng, D. M., Urch, J. E., ten Cate, J. M., Rao, V. A., van Aalten, D. M., and Crielaard, W. (2009) Streptococcus mutans SMU.623c codes for a functional, metal-dependent polysaccharide deacetylase that modulates interactions with salivary agglutinin. *J. Bacteriol. 191*, 394−402.
(37) Taylor, E. J., Gloster, T. M., Turkenburg, J. P., Vincent, F., Brzozowski, A. M., Dupont, C., Shareck, F., Centeno, M. S., Prates, J. A., Puchart, V., Ferreira, L. M., Fontes, C. M., Biely, P., and Davies, G. J. (2006) Structure and activity of two metal ion-dependent acetylxylan esterases involved in plant cell wall degradation reveals a close similarity to peptidoglycan deacetylases. *J. Biol. Chem. 281*, 10968−10975.
(38) Taylor, E. J., Gloster, T. M., Turkenburg, J. P., Vincent, F., Brzozowski, A. M., Dupont, C., Shareck, F., Centeno, M. S., Prates, J. A., Puchart, V., Ferreira, L. M., Fontes, C. M., Biely, P., and Davies, G. J. (2006) Structure and activity of two metal ion-dependent acetylxylan esterases involved in plant cell wall degradation reveals a close similarity to peptidoglycan deacetylases. *J. Biol. Chem. 281*, 10968−10975.